Journal Pre-proof

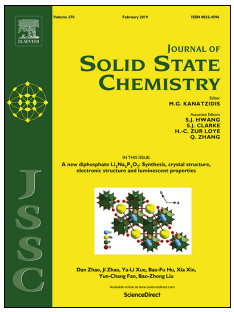

Selective cationic dye sorption in water by a two-dimensional zinc-carboxylate coordination polymer and its melamine-formaldehyde foam composite

Mohammad Alizadeh Bavieh, Valiollah Nobakht, Tahereh Sedaghat, Lucia Carlucci, Pierluigi Mercandelli, Mehdi Taghavi

PII: S0022-4596(20)30686-1

DOI: https://doi.org/10.1016/j.jssc.2020.121855

Reference: YJSSC 121855

To appear in: *Journal of Solid State Chemistry*

Received Date: 4 September 2020

Revised Date: 7 November 2020

Accepted Date: 9 November 2020

Please cite this article as: M.A. Bavieh, V. Nobakht, T. Sedaghat, L. Carlucci, P. Mercandelli, M. Taghavi, Selective cationic dye sorption in water by a two-dimensional zinc-carboxylate coordination polymer and its melamine-formaldehyde foam composite, *Journal of Solid State Chemistry* (2020), doi: https://doi.org/10.1016/j.jssc.2020.121855.

Credit Author Statement:

Mohammad Alizadeh Bavieh:

Formal analysis, Methodology, Writing - Original Draft, Writing - Review & Editing, software, Investigation

Valiollah Nobakht:

Conceptualization, Writing - Original Draft, Writing - Review & Editing, Validation, Resources, Data curation, Supervision, Project administration, Funding acquisition

Tahereh Sedaghat:

Resources, Writing - Review & Editing, Funding Aquisition, Supervision

Lucia Carlucci:

Data curation, Formal Analysis, Funding Aquisition, Investigation, Project administration, Resources, Software, Writing – editting & review

Pierluigi Mercandelli:

Data curation, Formal Analysis, Funding Aquisition, Investigation, Project administration, Resources, Software, Writing – editting & review

Mehdi Taghavi:

Resources, Writing - Review & Editing

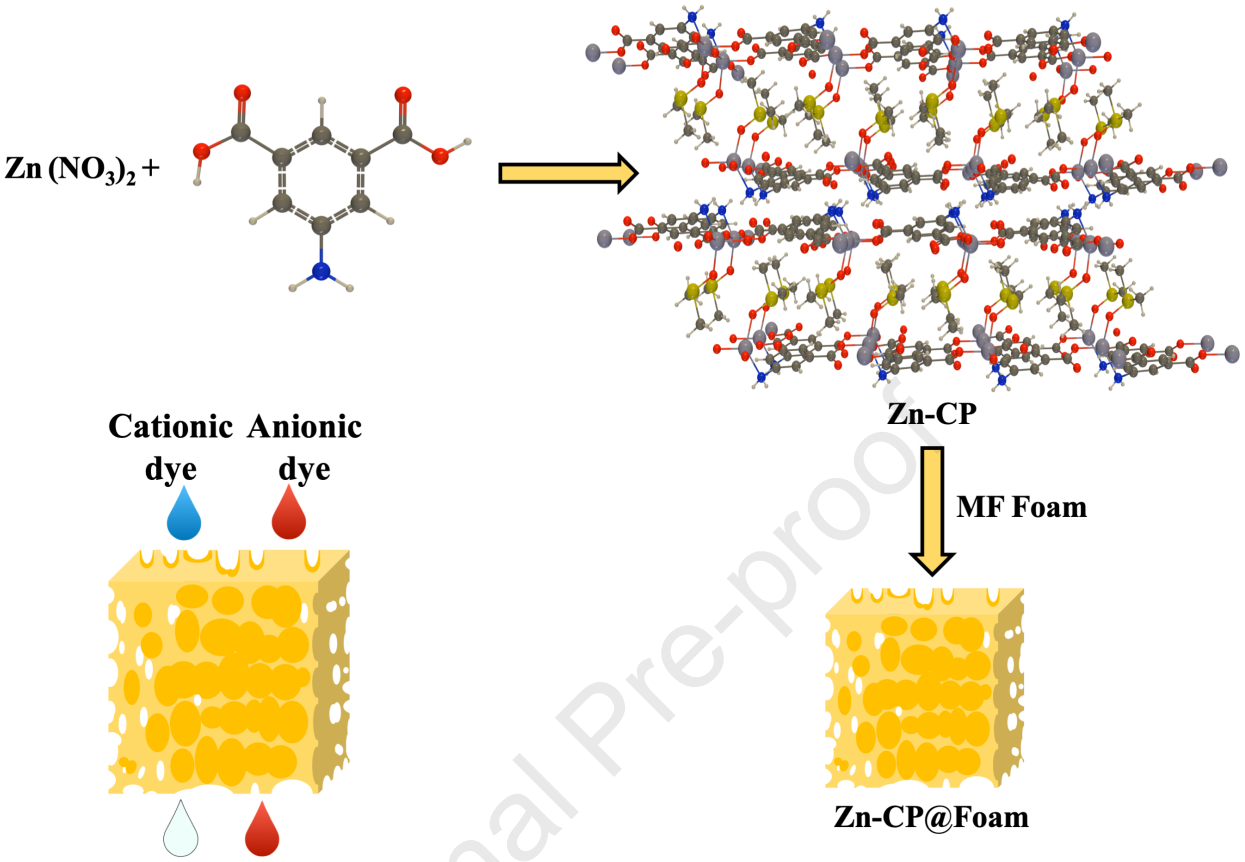

Selective cationic dye sorption in water by a two-dimensional zinc-carboxylate coordination polymer and its melamine-formaldehyde foam composite

Mohammad Alizadeh Bavieh, [a] Valiollah Nobakht, [a,*] Tahereh Sedaghat, [a] Lucia Carlucci, [b] Pierluigi Mercandelli, [b] Mehdi Taghavi [a]

[a] Department of Chemistry, Faculty of Sciences, Shahid Chamran University of Ahvaz, Ahvaz, Iran.

[b] Dipartimento di Chimica, Università degli Studi di Milano, via Camillo Golgi 19, 20133 Milano, Italy.

* Corresponding author. *E-mail address:* v.nobakht@scu.ac.ir (V. Nobakht).

ABSTRACT

A new two-dimensional zinc(II) coordination polymer of 5-aminoisophtalic acid (H_2AIP), namely [Zn(AIP)(DMSO)]$_n$ (**Zn-CP**), has been successfully prepared *via* conventional heating at 100°C in a (2:1) dimethyl sulfoxide/ethanol solvent mixture. The compound has been characterized by FT-IR spectroscopy, elemental and thermogravimetric analyses, powder and single-crystal X-ray diffraction techniques. Crystal structure of **Zn-CP** shows the presence of neutral layers of composition Zn(AIP) and **6^3-hcb** topology, which are decorated only on one side with dangling DMSO molecules. Moreover, the composite **Zn-CP@Foam** has also been fabricated growing **Zn-CP** crystals on the 3D porous structure of a melamine-formaldehyde foam (MF) by immersion of pieces of MF in the precursor solution of the coordination polymer. Both **Zn-CP** and **Zn-CP@Foam** materials have been studied for the adsorption in water of cationic dyes, such as Crystal Violet (**CV**), Victoria Blue (**VB**) and Malachite Green (**MG**), and anionic dyes, such as Sunset Yellow (**SY**), Congo Red (**CR**) and Aniline Blue (**AB**). Results show selective sorption of cationic dyes only, with faster and larger adsorption capacity observed for the porous composite material which has an adsorption capacity for Victoria Blue (**VB**) (102 mg g^{-1}) more than twice larger than that found for pristine **Zn-CP** powder (48 mg g^{-1}). This selectivity towards cationic dyes is attributed to electrostatic interactions between the cationic dye molecules and the negatively charged surface of the zinc coordination polymer, which shows a zeta potential of –13.7 mV. Moreover, dye adsorbed **Zn-CP** and **Zn-CP@Foam** can be regenerated by immersion–in water/acetic acid solution (1:1) and reused with almost the same efficiency.

***Keywords*:** Zinc Coordination Polymer; Melamine Formaldehyde Foam; Functional Composite, Dye Adsorption; 5-Aminoisophtalic Acid

1 INTRODUCTION

Organic dyes as essential textile industrial compounds are widely applied to wool, silk, and nylon fibers manufacturing [1]. Wastewaters produced by these industrial activities, therefore, contain dyes and pigments which, being harmful to ecosystems and human health, need to be efficiently removed [2]. So far, physical adsorption, biological and chemical treatments, among other methods, have been developed to treat waters polluted by dyes [3–5]. The adsorption of organic dyes in water by zeolites and activated carbon is a cost-effective method on an industrial scale [6]. However, the development of new materials, more efficient and selective in dye adsorption, is of significant importance from the standpoint of the environment. In this context, inorganic-organic hybrid materials, including coordination polymers (CPs) and metal-organic frameworks (MOFs) are excellent candidates [7–8]. CPs and MOFs, thanks to their tailored and tunable structures and easy variability in chemical compositions, which have been obtained *via* various synthetic methods [9-11], have attracted great interest and have found potential applications in many fields, including gas storage and separation, catalysis, drug delivery, sensing, and pollutants adsorption [12–16]. In adsorption-related applications, the topology and the chemical functionalization of the structures of CPs and MOFs, as well as the formation of composite materials, have been exploited to allow the selective adsorption of guest molecules such as organic dyes and other polluting materials [17–22]. Usually, interactions such as hydrogen bonding, electrostatic, acid-base, C–H···π and π···π stacking govern the relation of the guest molecules with CPs and MOFs as host [23, 24]. In this regard, preferential sensing, separation or adsorption of molecules could be driven by the strength of such host-guest interactions. Moreover, additional interactions between CPs or MOFs and guest molecules, involving unsaturated metal sites and functionalized ligands, have rendered these materials superior to other porous and non-porous adsorbents for efficient adsorptive removal of hazardous compounds from the air or aqueous phases. As reported in the literature, CPs constructed by different linkers and Co(II), Cu(II), Zr(IV), Zn(II), Mo(VI), Fe(III), Al(III), Cd(II), and also lanthanide metal centers have been investigated as adsorbents and some of them can be used for

selective adsorption of organic dyes on the base of size exclusion or electrostatic effects [25–28]. In addition to the adsorptive removal method, photocatalytic degradation of dye molecules in the presence of metal-organic materials is another way for the removal of dye pollutants from the effluents [29-32].

Despite of that, one of the issues to use these materials as an adsorbent is their hard separation from the application systems. However, concurrent development of metal-organic composites with a variety of functional materials, such as organic polymers, magnetic metal oxides, metal nanoparticles, quantum dots, polyoxometalates, carbon derivatives and biomolecules, has significantly enhanced the properties and applications of CPs and MOFs that are superior to those of the pristine components [33-36]. Polymeric organic foams, with their good characteristics such as cheapness, low toxicity to the environment, and suitable physico-chemical stability, can help to overcome the obstacle of hard separation through the fabrication of foam/CPs composites. Moreover, in addition to provide a stable and easily removable support to CPs, the three-dimensional porous structure of the foam composite allows a better mass transfer, giving a more effective sorption behavior.

Taking into account the aforementioned points, in this work we have synthesized and characterized a new two dimensional zinc(II) coordination polymer of 5-aminoisophthalic acid (H_2AIP), namely $[Zn(AIP)(DMSO)]_n$ (**Zn-CP**). In addition, its melamine-formaldehyde foam (MF) composite (**Zn-Cp@Foam**) has been successfully prepared and characterized. The capability in dye adsorption of both pristine **Zn-CP** and **Zn-CP@Foam** composite has been evaluated in water, revealing the ability of these materials to selectively adsorb cationic dyes.

2 EXPERIMENTAL SECTION

2.1 Materials and instrumentation

All experiments were carried out in air. All materials and solvents were purchased from commercial sources and used without further purification. Infrared spectra (4000−400 cm^{-1}) were recorded from KBr disks with a Perkin Elmer Spectrum Two FT-IR spectrometer. CHNS elemental analysis was performed on an Elementar Vario EL III CHNS analyzer. Thermogravimetric analysis (TGA) was carried out on a STA PT1600 (Linseis) thermal analyzer at a heating rate of 10°C min^{-1} under N_2 atmosphere in the temperature range of 50–800 °C.

Electronic spectra were recorded on a GBC Cintral 101 UV-Vis spectrophotometer. Powder X-ray diffraction (PXRD) patterns were recorded on a Philips X'PertPro diffractometer (Cu Kα radiation, λ = 1.54184 Å) in the 2θ range 5−50°. Zeta potentials were measured by the Malvern ZETASIZER ZEN3600 with the liquid concentration of 50 ppm. Scanning electron microscope (SEM) images were obtained using a LEO 1455VP apparatus. Simulated PXRD pattern of **Zn-CP** was obtained from single-crystal X-ray diffraction data using Mercury [37]. Topological analysis was performed using ToposPro [38].

2.2 Synthesis of [Zn(AIP)(DMSO)]$_n$ (Zn-CP)

0.30 g (1.0 mmol) of $Zn(NO_3)_2 \cdot 6H_2O$ and 0.18 g (1.0 mmol) of 5-aminoisophtalic acid (H_2AIP) were separately dissolved in 20 mL of a DMSO/ethanol (2:1) mixture. The two solutions were poured into a test tube, mixed thoroughly, and the resulting mixture was heated at 100°C in an oil bath. Colorless single crystals of **Zn-CP** suitable for X-ray diffraction analysis were grown by slow evaporation of the solvents, under heating, in about 4 days. The crystals were collected by filtration, washed with DMSO/ethanol, and then dried in air (0.21 g, 65% yield based on Zn). Anal. Calcd for $C_{10}H_{11}NO_5SZn$ (%): C, 37.22; H, 3.43; N, 4.34; S, 9.93. Found (%): C, 37.18; H, 3.74; N, 4.56; S, 9.96. FT-IR (cm^{-1}): 3140 and 3248 (-NH_2), 1344–1368 (-COO, sym), 1574–1628 (-COO, asym).

2.3 Fabrication of the composite Zn-CP@Foam

0.89 g (3.0 mmol) of $Zn(NO_3)_2 \cdot 6H_2O$ and 0.55 g (3.0 mmol) of H_2AIP were dissolved in 50 mL of a DMSO/EtOH (2:1) mixture and stirred for 30 min at RT to afford the precursor solution. Then, several pieces of a melamine-formaldehyde foam (MF) with dimensions of 5×5×5 mm^3 were activated by sonication in EtOH for 30 min and successively dried. The foam pieces were fully immersed into the precursor solution and heated at 100°C in an oil bath for 2 days. The supernatant solution was removed and the spare solution was absorbed by non-woven fabric. The resulting **Zn-CP@Foam** pieces were dried at 80°C for 24 h. During this process, crystals of **Zn-CP** were grown on the surface of the foam skeleton, leading to loading of about 650% (obtained by gravimetric analysis).

2.4 Dye adsorption and release

To increase the surface area of the adsorbent, the crystals of **Zn-CP** were ground in an agate mortar before dye adsorption experiments. 10.0 mg of well ground crystals of **Zn-CP** or 24.0 mg of **Zn-CP@Foam** were poured into 10 mL of dye solutions with distinct concentration (**MG** 40, **CV** 10, **VB** 15, **SY** 50, **AB** 90, **CR** 40 ppm) and then stirred at room temperature (10 min for cationic dyes and 180 min for anionic dyes). The solids were separated by centrifugation and the supernatants were used to determine the adsorption rate by UV-Vis spectroscopy. The absorbance was measured at 590, 600, 617 nm for cationic dyes Crystal Violet (**CV**), Victoria Blue (**VB**), and Malachite Green (**MG**), and at 484, 497 and 605 nm for anionic dyes Sunset Yellow (**SY**), Congo Red (**CR**), and Aniline Blue (**AB**), respectively.

To release adsorbed dye molecules and to recover the adsorbents, the used **Zn-CP** or **Zn-CP@Foam** composite were washed thoroughly with a mixed water/acetic acid (1:1) solution (3×5 mL). The recovered adsorbents were then washed with water and dried in air.

2.5 Single-crystal X-ray diffraction analysis

X-ray data were collected on a Bruker Apex II diffractometer using Mo *K*α radiation (0.71073 Å). The structures were solved using direct methods and refined using a full-matrix least-squares procedure based on F^2, using all data [39]. Hydrogen atoms were placed at geometrically estimated positions. The dimethyl sulfoxide ligand is disordered over two positions. The two overlapping images were refined applying soft restraints on bond distances and bond angles, based on the mean values obtained from a survey of the Cambridge Structural Database. Details relating to the crystals and the structural refinements are presented in Table 1, while a list of relevant distances and angles can be found in Table 2, together with the definition of all the symmetry-equivalent positions used in the structural description. Full details of crystal data and structure refinement are available as Supporting Information in CIF format. CCDC 2011679 contains the supplementary crystallographic data for **Zn-CP**.

3 RESULTS AND DISCUSSION

3.1 Crystal structure of $[Zn(AIP)(DMSO)]_n$ (Zn-CP)

Single crystals of **Zn-CP** suitable for X-ray diffraction analysis were obtained from an equimolar solution of H_2AIP and $Zn(NO_3)_2{\cdot}6H_2O$ in DMSO/ethanol (2:1) after heating at 100°C and

successive cooling at RT. The compound crystallizes in the monoclinic $P2_1/c$ space group with Z = 4 (Table 1) and exhibits a 2D layered structure. The asymmetric unit contains one Zn(II) cation, one AIP^{2-} anion, and one coordinated DMSO solvent molecule (Figure 1a). Each zinc ion is coordinated by three oxygen and one nitrogen atoms from three distinct AIP^{2-} ligands in addition to an oxygen atom from the coordinated DMSO molecule, adopting a ZnO_4N coordination environment. The coordination geometry of zinc center lies between square-pyramidal (SPY) and trigonal-bipyramidal (TBPY) with a calculated index of trigonality τ_5 of 0.6 (τ_5 = 0 or 1 for ideal SPY or TBPY, respectively) [40].

Each AIP^{2-} anion interact with three zinc atoms through the amino group (Zn–N 2.0501(12) Å) and the two carboxylic groups, one chelating (Zn–O 1.9934(10) and 2.5743(12) Å) and one monodentate (Zn–O 1.9307(11) Å) (respectively, 1.11 and 1.10 according to the Harris notation [41]). Connection of Zn(II) centers *via* μ_3-AIP^{2-} linkers generate layers which extend in the **bc** plane and have $\mathbf{6^3}$**-hcb** topology [42-44] (3-c nodes are, alternately, zinc atoms and AIP^{2-} centroids) (Figure 1b). Coordinated DMSO-κ^1*O* molecules (Zn–O 1.9702(12) Å) decorate only one side of the sheets and, being two neighboring sheets oriented in opposite direction and slipped in relation to each other, DMSO accommodates in the interlayer region by interdigitation (Figure 1c). Single layers pack *ABAB* along the **a*** direction to give the bi-layer motifs described above, which stack in the same direction with an *AAAA* arrangement.

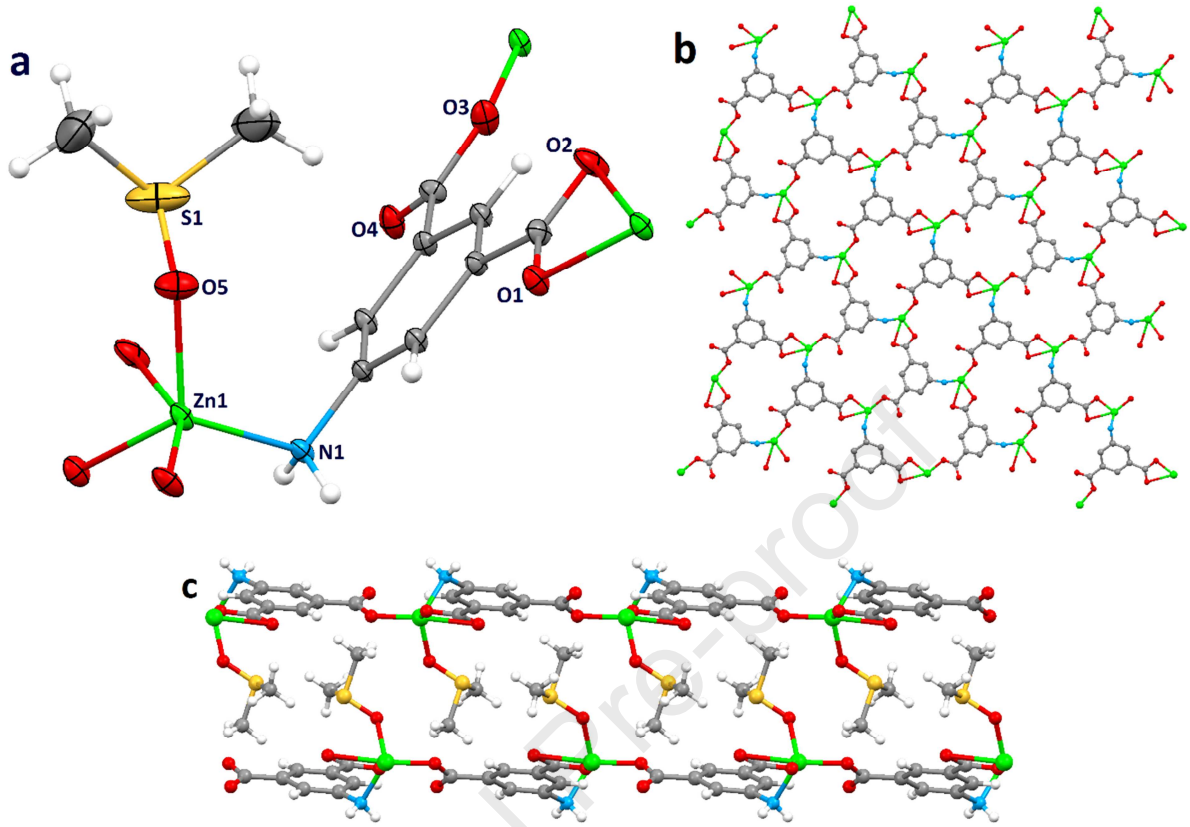

Figure 1. The structure of $[Zn(AIP)(DMSO)]_n$ (**Zn-CP**). (a) Asymmetric unit with additional atoms to complete the coordination environment of the zinc atom. (b) A single 2D sheet extending in the **bc** plane and with $\mathbf{6^3}$**-hcb** topology. DMSO molecules and hydrogen atoms were omitted for clarity. (c) View of the interdigitation between two adjacent sheets, which pack in *ABAB* mode along **a***. Interdigitating DMSO molecules are disordered and the major component only is here shown for clarity.

In addition to coordinative bonds generating the 2D layers, weak interactions are also present between neighboring interdigitated bi-layers motifs, which extend the structure to a supramolecular 3D framework. In particular, these interactions are hydrogen bonds between amino N–H groups and oxygen atoms of carboxylate groups belonging to neighboring bi-layers motifs (N1···O1^{iii} 3.0210(16) and N1···O4^{iv} 2.9851(17) Å), and π···π interactions involving aromatic rings of linkers belonging likewise to adjacent bi-layers (distance between centroids 3.8997(11) Å, distance between least-squares planes 3.2799(5) Å, slippage 2.109(3) Å; the rings are defined by atoms C1–C6 and C1^{v}–C6^{v}).

The $[Zn(AIP)(DMSO)]_n$ (**Zn-CP**) reported here is analogous to the already reported structures $[Zn(AIP)(solvent)]_n$ in which solvent = H_2O (refcode: UFULEM) [45], *N*,*N*-diethylformamide (DEF) (refcode: OCEYAX) [46], and *N*,*N*-dimethylacetamide (DMA) (refcode: CIFBUQ) [47]. This confirms that the 2D layer $[Zn(AIP)]_n$ with **hcb** topology can be obtained in different synthetic conditions and is the preferred reaction product in the presence of coordinating solvent molecules. The structural features of the $[Zn(AIP)]_n$ layers are essentially the same in all the structures [48], while what is different is the interlayer distance within the bi-layers motifs which is dictated by the volume of the different solvent molecules. Interlayer distances for $[Zn(AIP)(solvent)]_n$, computed as the distance between the planes defined by the zinc atoms contained in the two layers, are 2.43, 5.68, 6.13, and 7.25 Å for solvent = H_2O, DMSO, DMA and DEF, respectively (Figure 2).

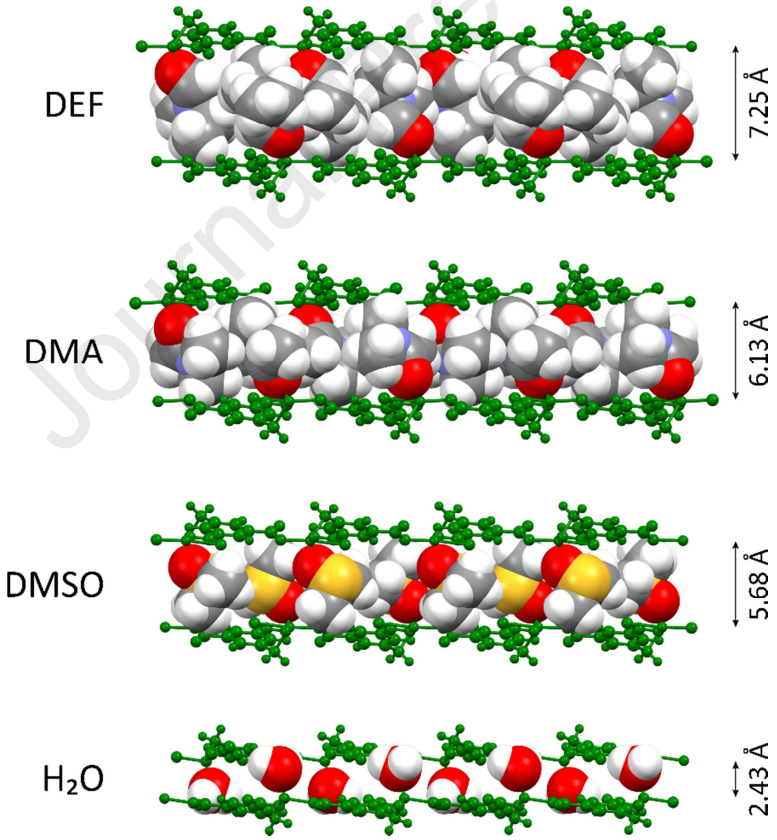

Figure 2. Interlayer distances in the four related structures $[Zn(AIP)(solvent)]_n$. From top to bottom: solvent = *N*,*N*-diethylformamide (DEF), *N*,*N*-dimethylacetamide (DMA), dimethyl sulfoxide (DMSO), and water.

Table 1. Crystallographic data and structure refinement details for **Zn-CP**.

	Zn-CP
Formula	$C_{10}H_{11}NO_5SZn$
Formula mass	322.65
T (K)	150(2)
Crystal system	monoclinic
Space group	$P2_1/c$
a (Å)	9.8364(16)
b (Å)	7.6758(13)
c (Å)	16.125(3)
β (°)	95.100(2)
V (Å^3)	1212.7(4)
Z	4
D_{calcd} (g cm^{-3})	1.767
No. of reflns collected	15083
No. of independent reflns	3824
No. of observed reflns	3434
R_{int}	0.0201
$(\sin\theta/\lambda)_{max}$ (Å^{-1})	0.739
Data / restraints / params	3824 / 86 / 193
S (all data)	1.097
R_1 [$I > 2\sigma(I)$]	0.0249
wR_2 (all data)	0.0673

Table 2. Selected bond lengths (Å) and angles (˚) for **Zn-CP**.

Bond Lengths (Å)			
Zn1–N1	2.0501(12)	Zn1–O3^{ii}	1.9307(11)
Zn1–O1^{i}	1.9934(10)	Zn1–O5	1.9702(12)
Zn1–O2^{i}	2.5743(12)		
Bond Angles (˚)			
N1–Zn1–O1^{i}	105.00(5)	O1^{i}–Zn1–O3^{ii}	101.82(4)
N1–Zn1–O2^{i}	81.81(4)	O1^{i}–Zn1–O5	120.80(5)
N1–Zn1–O3^{ii}	114.39(5)	O2^{i}–Zn1–O3^{ii}	156.83(4)
N1–Zn1–O5	114.85(5)	O2^{i}–Zn1–O5	87.33(4)
O1^{i}–Zn1–O2^{i}	56.43(4)	O3^{ii}–Zn1–O5	99.47(5)

Superscripts i–v indicate atoms generated by the following symmetry operations: (i) x, $-1 + y$, z; (ii) x, ½ – y, –½ + z; (iii) $-x$, – ½ + y, 1½ – z; (iv) $-x$, $-y$, 2 – z; (v) $-x$, 1 – y, 2 – z.

3.2 Synthesis and characterization

The new **Zn-CP** was synthesized by reacting H_2AIP and $Zn(NO_3)_2{\cdot}6H_2O$ in a DMSO/ethanol (2:1) mixture under conventional heating at 100°C. The **Zn-CP@Foam** composite was prepared

via immersion of MF pieces in the **Zn-CP** precursor solution and subsequent heating at 100°C (Figure 3a).

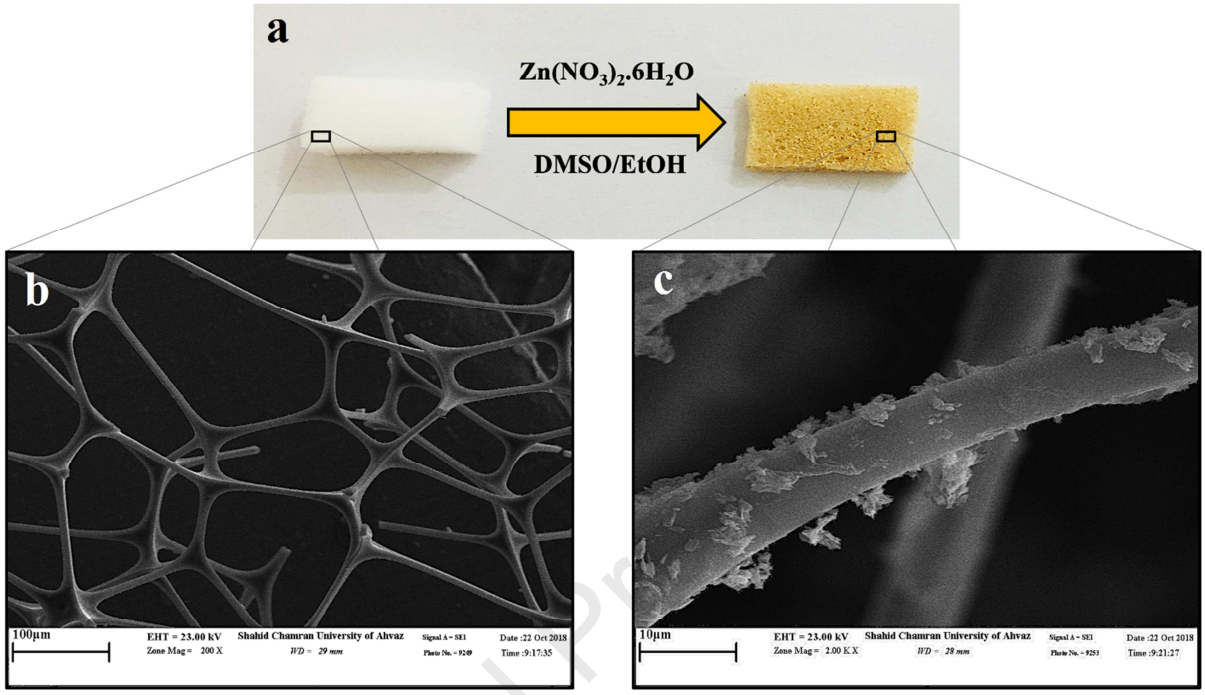

Figure 3. (a) Fabrication of the **Zn-CP@Foam** composite from the bulk MF foam and the **Zn-CP** precursor solution. SEM images of (b) the untreated MF foam and (c) the foam over which the **Zn-CP** microcrystals have been grown.

Phase purity of the as-synthetized **Zn-CP** and **Zn-CP@Foam** composite was checked by comparison of the experimental PXRD patterns with that simulated from single-crystal X-ray diffraction data. The good agreement between the three patterns confirms the purity and crystallinity of the samples, as well as the growth of **Zn-CP** on the surface of the MF foam (Figure 4).

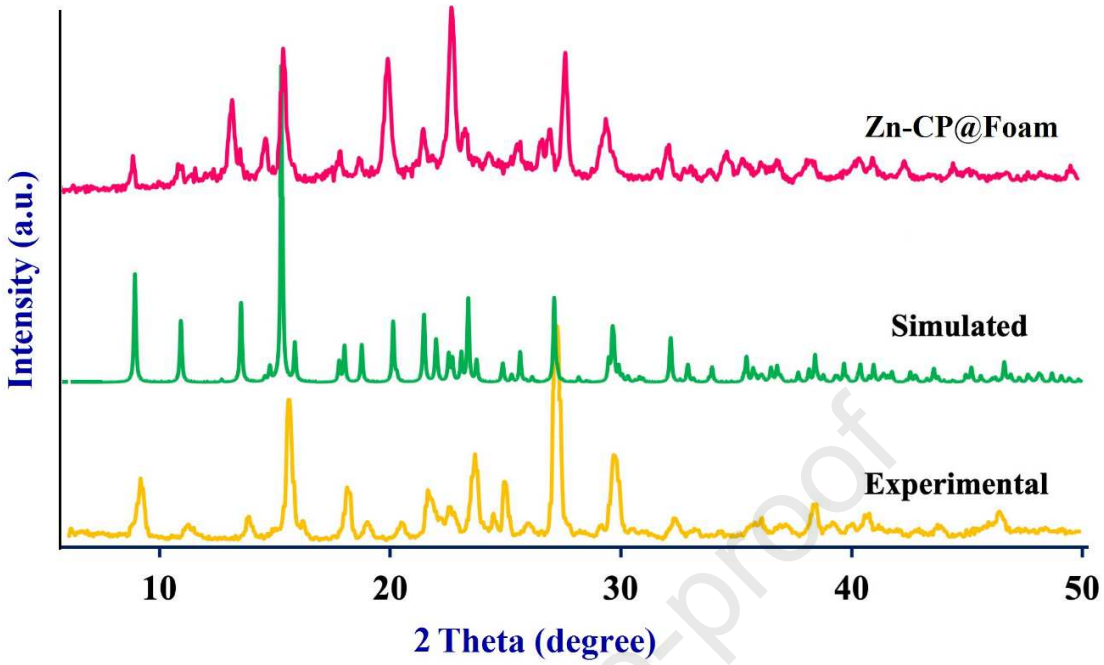

Figure 4. Comparison of the experimental PXRD patterns for **Zn-CP** (orange) and **Zn-CP@Foam** composite (magenta) with simulated pattern (green) from single-crystal data.

In the infrared spectrum of **Zn-CP** the absorption bands with weak to medium intensity in the range 2900–3100 cm^{-1} are assigned to the stretching vibrations of the aromatic C–H bonds of the AIP^{2-} ligand (Figure 5). The bands at 3140 and 3248 cm^{-1} are attributed to the stretching vibrations of the N–H bonds of the AIP^{2-}, as expected red-shifted (24 cm^{-1}) with respect to free H_2AIP [49]. The infrared spectrum of the **Zn-CP** also shows two intense bands in the ranges 1344–1368 and 1574–1628 cm^{-1} which are assigned to the symmetric and asymmetric stretching vibrations of carboxylate groups, respectively [50–51]. The peak at 1010 cm^{-1} may be attributed to the S=O stretching vibration of a DMSO molecule coordinated to a metal center by means of the oxygen atom [52]. Infrared spectrum of the **Zn-CP@Foam** composite is also shown in Figure 5. The presence of additional peaks in this case can be considered as an evidence of the coexistence of the coordination polymer and the MF foam in the composite structure.

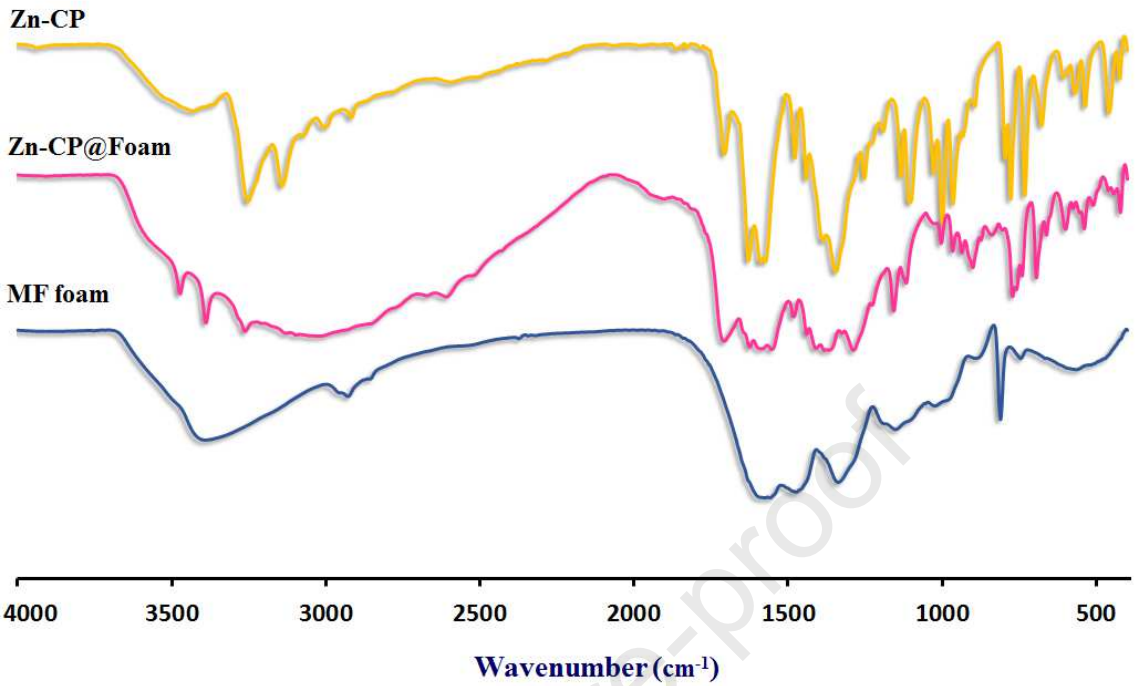

Figure 5. FT-IR spectra of the coordination polymer **Zn-CP** (orange) and the MF foam (blue) as separate phases and the **Zn-CP@Foam** composite (magenta).

Thermogravimetric analysis was performed to verify the thermal stability of **Zn-CP** (Figure S1). TG analysis of the $[Zn(AIP)(DMSO)]_n$ shows a small weight loss in the temperature range of 50-250 °C, attributed to the release of adsorbed water. The compound is stable up to about 250 °C. TG curve also show two main weight losses in the temperature range of 300-700 °C. The first loss of 24.2% in the range of 300-400 °C is consistent with the departure of DMSO solvents from the structure while the next loss of 50.5% in the range 400-700 °C is attributed to the combustion of the AIP^{2-} organic ligands. The residual weight of 25.3% is consistent with the formation ZnO.

SEM images of the MF foam and the **Zn-CP@Foam** composite have been recorded. As depicted in Figure 3b, the dominant morphology for the free MF foam is an open cell structure, with a large number of uniformly distributed and interconnected pores. Images of **Zn-CP@Foam** nicely confirm the deposition of microcrystals of **Zn-CP** on the surface of the MF foam substrate (Figure 3c).

3.3 Dye adsorption and release

Organic dyes can be classified according to many of their features, such as their structure, main chromophore, size, and ionic character. Taking into account the latter aspect, dyes can be distinguished into cationic and anionic and, to investigate the adsorption properties of **Zn-CP** and **Zn-CP@Foam** towards them, some representatives of the two categories were chosen and studied. Malachite Green (**MG**), Crystal Violet (**CV**), and Victoria Blue (**VB**) were selected among the cationic dyes, while Sunset Yellow (**SY**), Aniline Blue (**AB**), and Congo Red (**CR**) were selected among the anionic dyes. The adsorption experiments were performed according to the following procedure. Typically, a ground sample of **Zn-CP** (10 mg) was added into a vessel containing 10 mL of an aqueous solution of each organic dye at a given concentration (the initial dye concentration is detailed in the caption to Figure 6).

The supernatant solution was monitored by UV−Vis absorption spectroscopy at room temperature during a period of 180 min. After the addition of the **Zn-CP** adsorbent, only the color of the cationic dye solutions faded significantly, while the color of the anionic dye solutions remained unchanged along the whole experiment time (Figures 6 and 7).

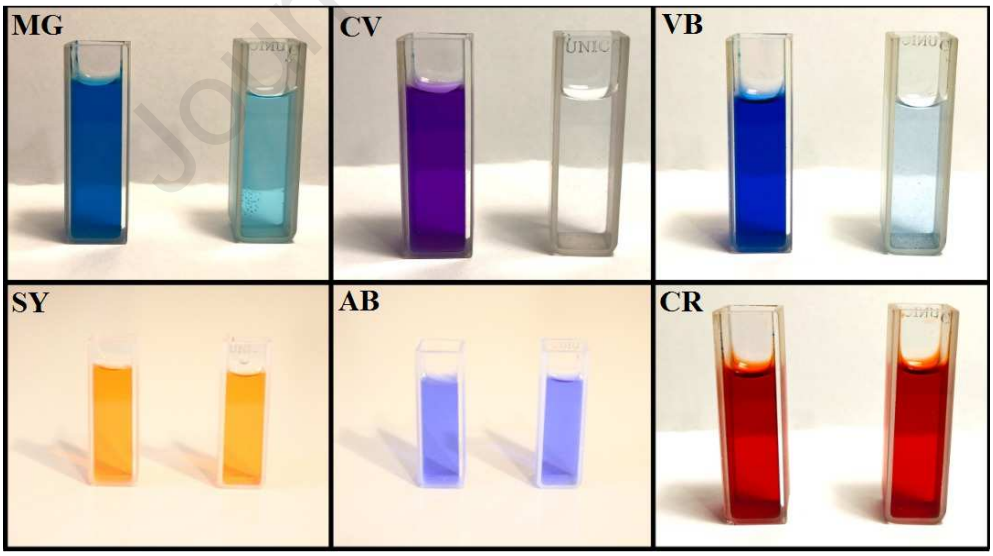

Figure 6. Photographs showing the color change of dye solutions before and after adsorption by **Zn-CP** (10 mg). Cationic dyes (up): Malachite Green (**MG**), Crystal Violet (**CV**), and Victoria Blue (**VB**). Anionic dyes (down): Sunset Yellow (**SY**), Aniline Blue (**AB**), and Congo Red

(**CR**). The initial concentration of the dye solutions (in ppm) are as follows: **MG** 40, **CV** 10, **VB** 15, **SY** 50, **AB** 90, **CR** 40.

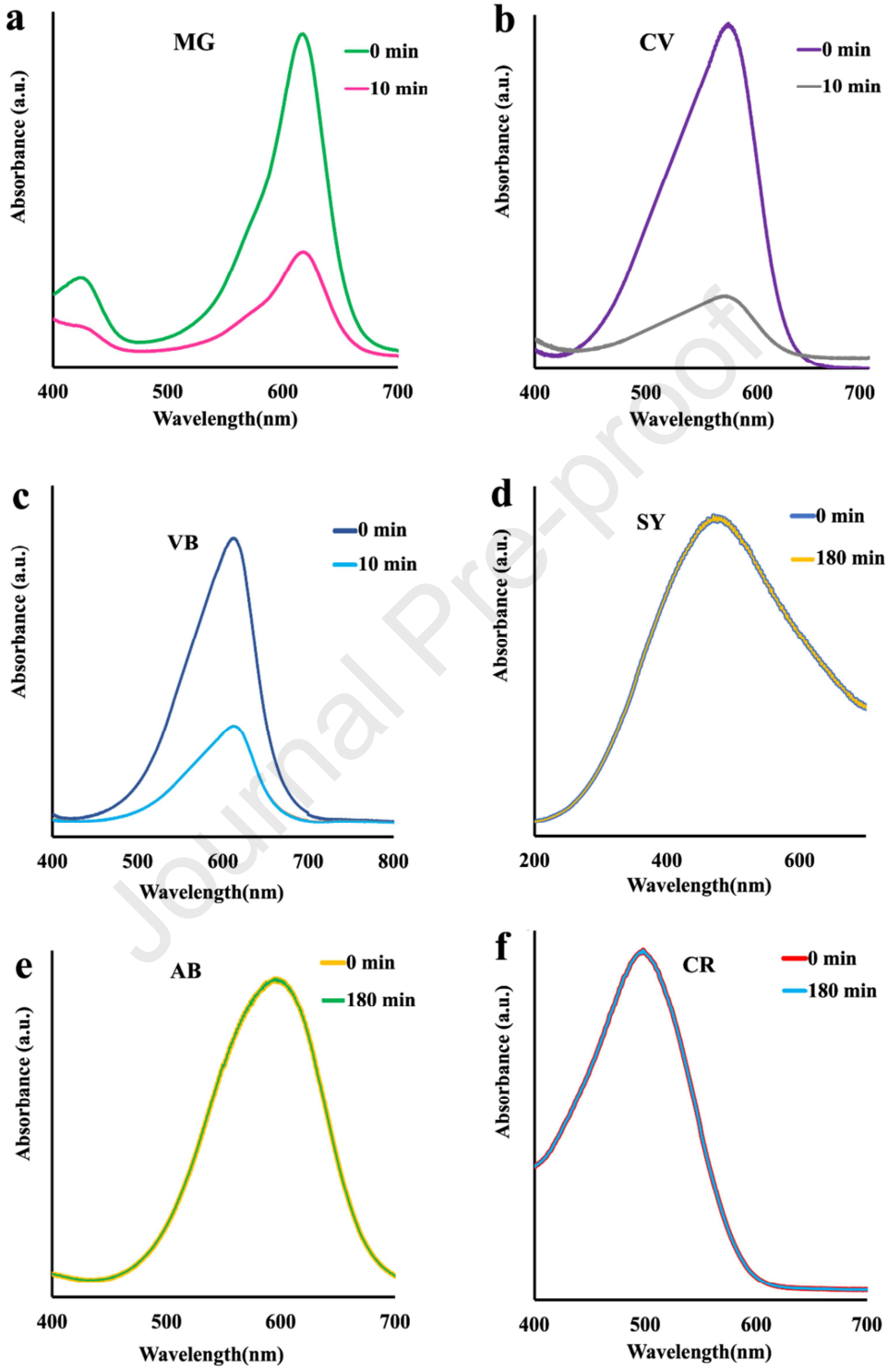

Figure 7. Absorption spectra of some dyes solutions before and after the addition of **Zn-CP** (10 mg). Cationic dyes (left column): (a) Malachite Green (**MG**), (b) Crystal Violet (**CV**), and (c)

Victoria Blue (**VB**). Anionic dyes (right column): (d) Sunset Yellow (**SY**), (e) Aniline Blue (**AB**), and (f) Congo Red (**CR**).

Various factors can play a role in the adsorption process, such as the size and shape of the dye molecules with respect to the porous structure of the adsorbent, as well as different types of adsorbent-adsorbate non-covalent interactions. Among these, electrostatic, π···π stacking, C–H···π, and hydrogen bond can have a significant impact on the adsorption mechanism of organic dyes by CPs and MOFs adsorbents. The selective adsorption of cationic dyes only on the **Zn-CP** surface indicates that, in this case, electrostatic interactions possibly rule the dye adsorption mechanism. Moreover, the large negative zeta potential measured for **Zn-CP** (–13.7 mV) supports the presence of a strong electrostatic interaction between the **Zn-CP** surface and the cationic dye species. The contribution of other factors can be tentatively ruled out since preliminary competition experiments, using structurally different cationic dyes, do not show significant differences in the adsorption amounts.

Given that Victoria Blue (**VB**) is adsorbed fast and in larger amount, it has been chosen to perform a detailed adsorption-desorption experiments. The quantity of the adsorbed organic dye at the equilibrium was calculated using the following equation:

$$Q_{\mathrm{eq}} = \frac{V(C_0 - C_t)}{m}$$

where Q_{eq} is the adsorption capacity or loading (the amount of adsorbate taken up by the adsorbent per unit mass of the adsorbent), C_0 is the initial concentration of the dye, C_t is the concentration of the dye at the equilibrium, V is the volume of the dye solution, and m is the mass of the soaked adsorbent. The calculated adsorption capacity of **Zn-CP** for **VB** is 48 mg g^{-1}.

To facilitate mass transfer during the adsorption process and hence enhance the efficiency of dye adsorption, **Zn-CP** has been grown on the surface of the 3D porous structure of a melamine-formaldehyde foam (*vide supra*). Foam substrates have proved to be excellent platforms for surface modification: this approach is simple, cost-effective and can be applied to fabricate various porous structures covered with selected CPs and MOFs, granting an enhanced mass transfer due to a larger surface area [53].

The obtained **Zn-CP@Foam** composite was tested in the adsorption of two cationic organic dyes in aqueous solution, namely Victoria Blue (**VB**) and Crystal Violet (**CV**). Results of the

adsorption experiments are depicted in Figure 8. The adsorption capacity of **Zn-CP@Foam** for **VB** is 102 mg g^{-1}, more than twice larger than that calculated for pristine **Zn-CP** powder. Percent adsorption efficiency values measured for **Zn-CP** and **Zn-CP@Foam** on the removal of **VB** from its aqueous solutions are 47% and 100%, respectively. The better performances of **Zn-CP@Foam** cannot be attributed to the foam only since its adsorption ability have been evaluated and proven to be negligible. Noticeably, the rate of **VB** adsorption by **Zn-CP@Foam** is much higher than that found for **Zn-CP** (compare Figure 8a and 8c). The different behavior of the two materials could be ascribed to the larger exposed surface area of the coordination polymer in the composite.

The adsorbed dye molecules could be also rapidly released in a water/acetic acid solution (1:1) after stirring the mixture for about 10 min, and the recovered adsorbent material can be reused with almost the same removal capacity.

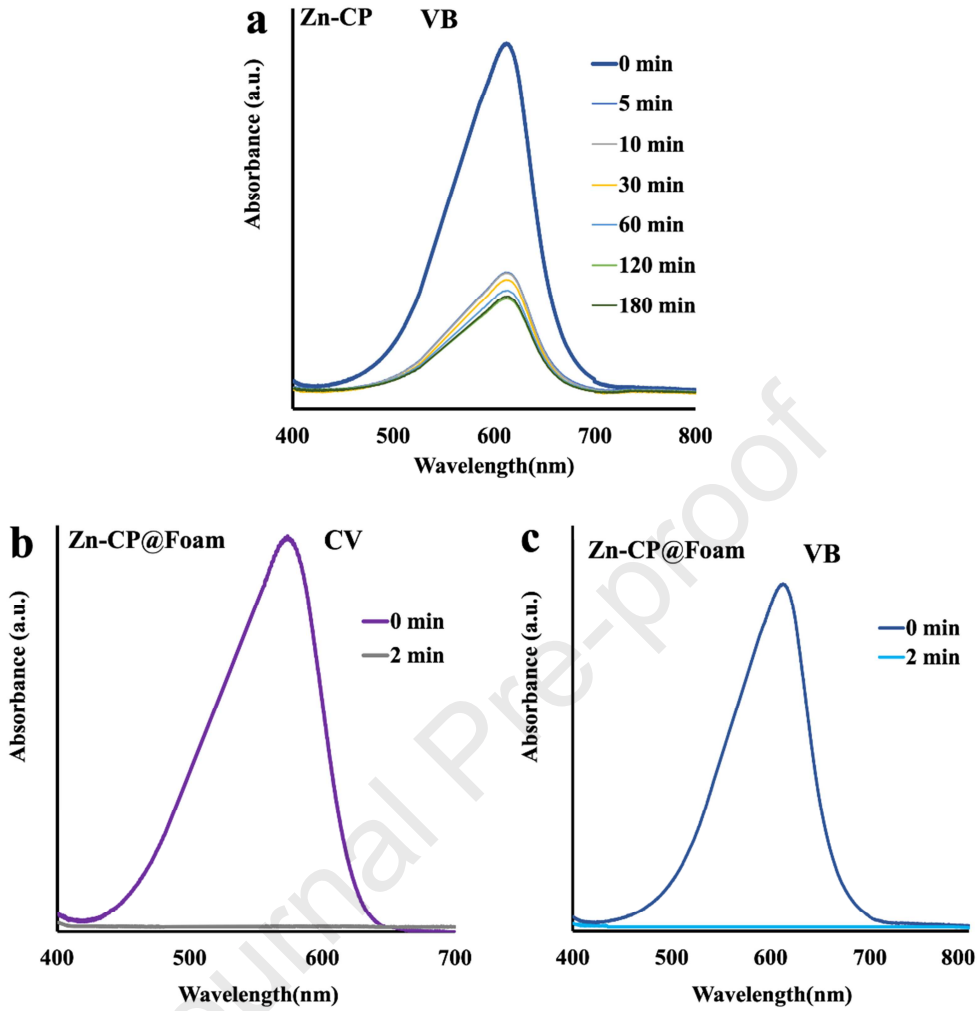

Figure 8. Temporal evolution of UV-Vis absorption spectra for (a) adsorption of **VB** (100 mL, 25 ppm) by **Zn-CP** (10 mg), (b) adsorption of **CV** (10 mL, 10 ppm) by **Zn-CP@Foam** (24 mg), and (c) adsorption of **VB** (10 mL, 15 ppm) by **Zn-CP@Foam** (24 mg).

4 CONCLUSION

The new 2D coordination polymer $[Zn(AIP)(DMSO)]_n$ (**Zn-CP**), containing 5-aminoisophtalic acid (H_2AIP), has been synthetized and characterized. Its crystal structure has been elucidated by single-crystal X-ray diffraction, revealing that this is a new derivative of the $[Zn(AIP)(solvent)]_n$ family (solvent = H_2O, DEF, and DMA). The present findings confirm the high stability of the two-dimensional motif Zn(AIP), that can be isolated under different synthetic conditions and stabilized by diverse solvent molecules. In addition, crystals of **Zn-CP** have been successfully grown on the highly porous 3D structure of a melamine-formaldehyde foam (MF) to produce the

composite **Zn-CP@Foam** material. Both materials have been proven to selectively adsorb only cationic dye molecules in aqueous solutions, with better performances for the porous composite **Zn-CP@Foam**. The negatively charged surface of **Zn-CP** (zeta potential of –13.7 mV) explains the selective removal of cationic dyes from water, while the porous structure of the composite material, with a larger exposed surface area, allows the removal of large amounts of dyes followed by an easy separation of the adsorbent from the solution. The composite provides a high capacity reversible adsorption/desorption behavior towards **VB** with a comparable performance to other well-known adsorbents such as fly ash, activated carbon, MCM-41, ZnO NPs, zeolites, and MOFs.

ACKNOWLEDGMENT

The authors thank Shahid Chamran University of Ahvaz (Grant No.: SCU.SC98.206) and the Università degli Studi di Milano (Piano di Sviluppo d'Ateneo, azione A, PSR2019_DIP_005_PI_LCAR) for financial support.

ORCID

Valiollah Nobakht https://orcid.org/0000-0002-8569-2602

Tahereh Sedaghat http://orcid.org/0000-0002-3352-1932

Lucia Carlucci https://orcid.org/0000-0001-5856-5280

Pierluigi Mercandelli https://orcid.org/0000-0002-9473-6734

Mehdi Taghavi https://orcid.org/0000-0002-6381-2845

REFERENCES

[1] X. S. Wang, J. Liang, L. Li, Z. J. Lin, P. P. Bag, S.Y. Gao, Y. B. Huang, R. Cao, Inorg. Chem. 55 (2016) 2641-2649.

[2] U. Roy, P. Das, A. Bhowal, S. Datta, Springer, Singapore, 2018, 187-193.

[3] S. Phengthaisong, A. Cheansirisomboon, J. Boonmak, S. Youngme, Inorg. Chim. Acta 479 (2018) 172-178.

[4] Q. Y. Zhai, J. Su, T. T. Guo, J. Yang, J. F. Ma, J. S. Chen, Cryst. Growth Des. 18 (2018) 6046-6053.

[5] H. Li, Q. Li, Y. He, N. Zhang, Z. Xu, Y. Wang, Materials 11 (2018) 744.

[6] R.-Z. Zhang, S. Quan, M. Xia, Q. Wang, W. Zhang, J.-M. Yang, J. Colloid Interface Sci. 525 (2018) 54-61.

[7] Y. Rachuri, S. Sreevalsa, P. Bhavesh, B. K. Kamal, S. Eringathodi, Dalton Trans. 47 (2018) 898-908.

[8] T. Zhang, G. Xiangyang, S. Yusheng, H. Cheng, D. Chunying, Nat. Commun. 9 (2018) 1-9.

[9] P. Li, F. F. Cheng, W. W. Xiong, Q. Zhang, Inorg. Chem. Front. 5 (2018) 2693-2708.

[10] W. W. Xiong, Q. Zhang, Angew. Chem. 54 (2015) 11616-11623.

[11] F. F. Cheng, J. N. Zhu, M. Y. Zhao, Z. J. Ma, W. W. Xiong, J. Solid State Chem. 278 (2019) 120904.

[12] L-Y. A. Lin, T. Wai-Chi, D. Yunchen, Chemosphere 195 (2018) 272-281.

[13] Y. Ma, L. Xiangyuan, L. Aijie, Y. Peng, Z. Caiyun, T. Bo, Angew. Chem. 56 (2017) 13752-13756.

[14] E. Baladi, V. Nobakht, A. Tarassoli, D. M. Proserpio, L. Carlucci. Cryst. Growth Des. 18 (2018) 7207-7218.

[15] C.Y. Gao, H. R. Tian, J. Ai, L. J. Li, S. Dang, Y. Q. Lan, Z. M. Sun, Chem. Comm. 54 (2018) 7093-7094.

[16] A. Tarassoli, V. Nobakht, E. Baladi, L. Carlucci, D. M. Proserpio, CrystEngComm 19 (2017) 6116-6126.

[17] H. R. Noormohamadi, M. R. Fat'hi, M. Ghaedi, V. Nobakht, S. Azizzadeh, Anal. Methods 11 (2019) 618-626.

[18] N.A Khan, Z. Hasan, S. H. Jhung, J. Hazard. Mater. 244 (2013) 444-456.

[19] Y. Belmabkhout, P. M. Bhatt, K. Adil, R. S. Pillai, A. Cadiau, A. Shkurenko, G. Maurin, G. Liu, W. J. Koros, M. Eddaoudi, Nat. Energy 3 (2018) 1059-1066.

[20] M. Yadollahi, H. Hamadi, V. Nobakht, J. Hazard. Mater. 399 (2020) 122872.

[21] S. Glomb, D. Woschko, G. Makhloufi, C. Janiak, ACS Appl. Mater. Interfaces 9 (2017) 37419-37434.

[22] S. Pan, R. Saha, S. Mandal, A. Gupta, M. A. Fernandez-Herrera, G. Merino, P. K. Chattaraj, J. Phys. Chem. C 120 (2016) 13911-13921.

[23] A. Beheshti, F. Hashemi, C. T. Abrahams, J. Taiwan Inst. Chem. Eng. 95 (2019) 504-514.

[24] H. R. Noormohamadi, M. R. Fat'hi, M. Ghaedi, S. Azizzadeh, V. Nobakht, J. Mol. Liq. 262 (2018) 71-77.

[25] J. Li, X. Wang, G. Zhao, C. Chen, Z. Chai, A. Alsaedi, T. Hayat, X. Wang, Chem. Soc. Rev. 47 (2018) 2322-2356.

[26] W.Y. Yin, T. T. Bian, J. Geng, Y. H. Hu, S. Q. Yan, X. Y. Tang, H. J. Cheng, Y.S. Ma, R. X. Yuan, Inorg. Chim. Acta 476 (2018) 1-6.

[27] X. Wang, J. Zhao, M. Le, H. Lin, J. Luan, G. Liu, X. Wang, J. Inorg. Organomet. Polym. Mater. 28 (2018) 800-804.

[28] J. Zhang, C. C. Wang, P. Wang, Y. L. Cao, RSC Adv. 6 (2016) 73595-73599.

[29] Q. Zhang, X. Jiang, A. M. Kirillov, Y. Zhang, M. Hu, W. Liu, L. Yang, R. Fang, W. Liu, ACS Sustain. Chem. Eng. 7 (2019) 3203-3212.

[30] K. Iqbal, A. Iqbal, A. M. Kirillov, B. Wang, W. Liu, Y. Tang, J. Mater. Chem. A, 5 (2017) 6716-6724.

[31] R. Kaur, K. Vellingiri, K. H. Kim, A. K. Paul, A. Deep, Chemosphere 154 (2016) 620-627.

[32] Y. Pan, Q. Ding, H. Xu, C. Shi, A. Singh, A. Kumar, J. Liu, CrystEngComm 21 (2019) 4578-4585.

[33] Q. L. Zhu, Q. Xu, Metal–organic framework composites. Chem. Soc. Rev. 43 (2014) 5468-5512.

[34] S. Li, F. Huo, Nanoscale 7 (2015) 7482-7501.

[35] Y. Chen, F. Chen, S. Zhang, Y. Cai, S. Cao, S. Li, W. Zhao, S. Yuan, X. Feng, A. Cao, X. Ma, J. Am. Chem. Soc. 139 (2017) 16482-16485.

[36] K. Zhang, Q. Huo, Y. Y. Zhou, H. H. Wang, G. P. Li, Y. W. Wang, Y. Y. Wang, ACS Appl. Mater. Interfaces 11 (2019) 17368-17374.

[37] Mercury 2020.1, Cambridge Crystallographic Data Centre, Cambridge, 2020.

[38] V. A. Blatov, A. P. Shevchenko, D. M. Proserpio, Cryst. Growth Des. 14 (2014) 3576–3586.

[39] G. M. Sheldrick, Acta Crystallogr., Sect. C: Struct. Chem. 71 (2015) 3–8.

[40] A. W. Addison, T. N. Rao, J. Reedijk, J. van Rijn, G. C. Verschoor, J. Chem. Soc., Dalton Trans. (1984) 1349–1356.

[41] R. A. Coxall, S. G. Harris, D. K. Henderson, S. Parsons, P. A . Tasker, R. E. P. Winpenny, J. Chem. Soc., Dalton Trans. (2000) 2349–2356.

[42] S. W. Jaros, M. F. C. Guedes da Silva, J. Król, M. Conceição Oliveira, P. Smolenski, A. J. Pombeiro, A. M. Kirillov, Inorg. Chem. 55 (2016) 1486-1496.

[43] S. W. Jaros, M. F. C. Guedes da Silva, M. Florek, P. Smoleński, A. J. Pombeiro, A. M. Kirillov, Inorg. Chem. 55 (2016) 5886-5894.

[44] S. Azizzadeh, V. Nobakht, L. Carlucci, D. M. Proserpio, Polyhedron 175 (2020) 114236.

[45] C.-D. Wu, C.-Z. Lu, W.-B. Yang, H.-H. Zhuang, J.-S. Huang, Inorg. Chem. 41 (2002) 3302–3307.

[46] K. O. Kongshaug, H. Fjellvag, Inorg. Chem. 45 (2006) 2424–2429.

[47] S.-Y. Yang, H.-B. Yuan, X.-B. Xu, R.-B. Huang, Inorg. Chim. Acta 403 (2013) 53–62.

[48] All the species are isostructural. However, since the species with S = H_2O has been described in $P2_1/n$ (at variance with all the others, described in $P2_1/c$) its layers extend in the b(a – c) plane and pack along the **a*** + **c*** direction.

[49] J. Jiang, Y. Lu, J. Liu, Y. Zhou, D. Zhao, C. Li, J. Solid State Chem. 283 (2020) 121153.

[50] J. M. Seco, S. Pérez-Yáñez, D. Briones, J. Á. García, J. Cepeda, A. Rodríguez-Diéguez, Cryst. Growth Des. 17 (2017) 3893−3906.

[51] S. Gholamali Ghomshehzadeh, V. Nobakht, N. Pourreza, P. Mercandelli, L. Carlucci, Polyhedron 176 (2020) 114265.

[52] M. Calligaris, Coord. Chem. Rev. 248 (2004) 351–375.

[53] H. Li, M. Li, W. Li, Q. Yang, Y. Li, Z. Gu, Y. Song, Phys. Chem. Chem. Phys. 19 (2017) 5746-5752.

A neutral layered zinc(II) coordination polymer (**Zn-CP)** has been synthesized, characterized, and successfully grown on the surface of the 3D porous structure of melamine-formaldehyde foam (MF) to fabricate a new porous **Zn-CP@Foam** composite. Both **Zn-CP** and **Zn-CP@Foam** materials show selective sorption of cationic dyes only, due to the negatively charged surface of the materials, with faster and larger adsorption capacity for the porous composite.

Highlights:

A new 2D zinc-coordination polymer (**Zn-CP**) has been successfully prepared and characterized

The compound show selective sorption of cationic dyes

A highly porous composite of melamine-formaldehyde foam and **Zn-CP** has also been fabricated

The composite has an adsorption capacity more than twice larger than that of pristine **Zn-CP**

Declaration of interests

☒ The authors declare that they have no known competing financial interests or personal relationships that could have appeared to influence the work reported in this paper.

☐The authors declare the following financial interests/personal relationships which may be considered as potential competing interests: